Development of Shallow Viscous Oil Reserves in North Slope

ID Number: DE-FC26-01BC15186

Quarterly Progress Report

Reporting Period Start Date: 4-1-2003

Reporting Period End Date: 6-30-2003

Submitted to the

U.S. Department of Energy

Kishore K. Mohanty

Department of Chemical Engineering

University of Houston

4800 Calhoun Road

Houston, Texas 77204-4004

July, 2003

Disclaimer

This report was prepared as an account of work sponsored by an agency of the United States Government. Neither the United States Government nor any agency thereof, nor any of their employees, makes any warranty, express or implied, or assumes any legal liability or responsibility for the accuracy, completeness, or usefulness of any information, apparatus, or process disclosed, or represents that its use would not infringe privately owned rights. Reference herein to any specific commercial product, process, or service by trade name, trademark, manufacturer, or otherwise does not necessarily constitute or imply its endorsement, recommendation, or favoring by the United States Government or any agency thereof. The views and opinions of authors expressed herein do not necessarily state or reflect those of the United States Government or any agency thereof.

Abstract

North Slope of Alaska has huge oil deposits in heavy oil reservoirs such as Ugnu, West Sak and Shrader Bluff etc. The viscosity of the last two reservoir oils vary from ~30 cp to ~3000 cp and the amount in the range of 10-20 billion barrels. High oil viscosity and low formation strength impose problems to high recovery and well productivity. Water-alternate-gas injection processes can be effective for the lower viscosity end of these deposits in West Sak and Shrader Bluff. Several gas streams are available in the North Slope containing NGL and CO_2 (a greenhouse gas). The goal of this research is to develop tools to find optimum solvent, injection schedule and well-architecture for a WAG process in North Slope shallow sand viscous oil reservoirs. In the last quarter, we added numerical solution along streamline subroutines to our streamline compositional simulator. The WAG injection algorithms are being developed. We studied the wettability of the reservoir oil and formulated a four-phase relative permeability model based on two-phase relative permeabilities. The effect of new relative permeability formulations on a five-spot pattern WAG recovery was evaluated. Effect of horizontal wells on pattern sweep has been initiated. A model quarter five-spot experiment is being designed. Plans for the next quarter includes modeling of WAG injection in streamline based simulation, evaluation of complex well-architecture and design of model quarter five-spot experiment.

TABLE OF CONTENTS

List of Graphical Materials

Executive Summary

North Slope of Alaska has huge oil deposits in heavy oil reservoirs such as Ugnu, West Sak and Shrader Bluff etc. The viscosity of the last two reservoir oils vary from ~30 cp to ~3000 cp and the amount in the range of 10-20 billion barrels. High oil viscosity and low formation strength impose problems to high recovery and well productivity. Water-alternate-gas injection processes can be effective for the lower viscosity end of these deposits in West Sak and Shrader Bluff. Several gas streams are available in the North Slope containing NGL and CO_2 (a greenhouse gas). The goal of this research is to develop tools to find optimum solvent, injection schedule and well-architecture for a WAG process in North Slope shallow sand viscous oil reservoirs. In the last quarter, we added numerical solution along streamline subroutines to our streamline compositional simulator. The WAG injection algorithms are being developed. We studied the wettability of the reservoir oil and formulated a four-phase relative permeability model based on two-phase relative permeabilities. The effect of new relative permeability formulations on a five-spot pattern recovery is being evaluated. Effect of horizontal wells on pattern sweep has been initiated. A model quarter five-spot experiment is being designed. Plans for the next quarter includes modeling of WAG injection in streamline based simulation, evaluation of complex well-architecture and design of model quarter five-spot experiment.

Introduction

North Slope of Alaska has huge oil deposits in heavy oil reservoirs such as Ugnu, West Sak and Shrader Bluff etc (Foerster et al., 1997). These reservoirs overlie existing productive reservoirs such as Kuparak and Milne Point. The viscosity of the West Sak and Shrader Bluff oils vary from ~30 cp to ~3000 cp and the amount is approximately 16 billion barrels. High oil viscosity and low formation strength impose problems to high recovery and well productivity. These challenging reservoirs are the largest undeveloped accumulations in North America. With even modest recoveries, reserves must be considered substantial (a few billion barrels).

Waterflood pilots have been attempted in both West Sak starting in 1984 and Shraeder Bluff in 1991 (Bidinger & Dillon., 1995). Initial well productivity of approximately 300 BOPD in a ~19 API oil is considered low by North Slope standards. The goal of this research is develop the new technology to increase the well productivity as well as the reservoir recovery efficiency. Water-alternate-gas injection processes and modern well architectures can be effective in recovery of the low viscosity (<100 cp) of these deposits in West Sak and Shredder Bluff. Several gas streams are available for the WAG process in the North Slope that contain NGL and CO_2. The disposal of (a few trillion cubic feet of) CO_2 will be an added benefit because CO_2 is a greenhouse gas and the sequestration of a significant amount of greenhouse gas is a challenge for the mankind in the twenty first century.

This report summarizes our results for the period of April 2003 through June 2003. The five tasks for the project are: (1) Compositional model, (2) Relative permeability, (3) Reservoir simulator, (4) Well Architecture, and (5) WAG optimization. Tasks 4 and 5 were initiated in this quarter; the activities are described in the next section.

Experimental

In our case studies (described in the next section), it was observed that during WAG floods many grid blocks had three phases: water (phase 1), oil (phase 2) and second liquid phase (phase 4). Some grid blocks had all four phases. Very few cells had water, oil and gas (phase 3). Therefore, in this work, the gas phase (phase 3) and the second liquid phase (phase 4) are treated as one combined pseudo-phase (g). In this section, the new four-phase relative permeability model is described in detail. We also introduce the case studies.

New Relative Permeability Model. The model is described in terms of its two-phase, three-phase and four-phase features.

Two-Phase Relative Permeability: Gas. We adopt the two-phase relative permeability for the gas phase proposed by Jerauld (1997), i.e.,

$$K_{rg} = \frac{(1+C_{g2})\,S_g^{*\,C_{g1}}}{1+C_{g2}S_g^{*\,C_{g1}(1+1/C_{g2})}}, \qquad (1)$$

where

$$S_g^* = \frac{S_g - S_{gt}}{1 - S_{gt} - S_{org} - S_{wr}}. \qquad (2)$$

Eq. 1 involves two parameters: C_{g1} and C_{g2}, which can be made functions of phase density for compositional consistency. If C_{g2} is assumed to be zero, then the gas relative permeability calculation is similar to that in the modified Corey model (Chang, 1990). It is apparent from the above equation that at low S_g values, the numerator dominates while at high S_g values, the second term in the denominator dominates. So the second term in the denominator can be treated as the contributions of the small pores to the relative permeability and is so designed that it gives a zero slope at $S_g = 1$. This is also consistent with the idea that the gas, being the most non-wetting

9

phase, enters the big pores first and then the smaller pores. The capillary number dependence is ignored because either gas or the second liquid displaces oil or is displaced by water.

Eq. 2 involves the term S_{gt} (trapped gas saturation). The trapped gas saturation influences the amount of miscible injectant (gas) retained in the reservoir that is not available for oil displacement. S_{gt} is defined as (Jerauld, 1997):

$$S_{gt}(S_g^{max}) = \frac{S_g^{max}}{1 + (1/S_{gr} - 1)S_g^{max\,1+b(S_{gr}/(1-S_{gr}))}}, \qquad (3)$$

where S_g^{max} is the maximum gas saturation that has occurred at that location at any time and b is empirically determined. This equation reduces to Land's equation when b equals 0 (Land, 1968). However, b should be less than or equal to 1 due to physical constraints. The above equation also satisfies the physical constraints: the trapped gas saturation is always less than S_g^{max} At high values of S_g^{max}, the trapped gas saturation approaches the residual gas saturation, S_{gr} while it approaches S_g^{max} at low S_g^{max} values. The problem associated with this model is that one has to keep track of maximum gas saturation in each grid block during simulation (but this can be easily handled). So it is possible that two grid blocks having the same gas saturation can have different permeabilities as they can have different S_g^{max}.

Two-Phase Relative Permeability: Oil. The oil relative permeabilities with respect to water and gas are given as:

$$K_{row} = K_{ro}^0 \left(\frac{S_o - S_{orw}}{1 - S_{wr} - S_{orw}} \right)^{C_{ow}} \qquad (4)$$

$$K_{rog} = K_{ro}^0 \left(\frac{S_o - S_{org}}{1 - S_{wr} - S_{org}} \right)^{C_{og}}, \qquad (5)$$

10

where S_{org}, S_{orw}, C_{ow} and C_{og} are functions of capillary number. At the miscible front in a multi-contact gas miscible process, the interfacial tension (IFT) becomes low resulting in high capillary number, which is needed to mobilize the residual oil in small pores. So, the change in IFT leads to changes in relative permeability.

Two-Phase Relative Permeability: Water. The water relative permeabilities with respect to oil and gas are calculated as,

$$K_{rwo} = K_{rw}^0 \left(\frac{S_w - S_{wr}}{1 - S_{wr} - S_{orw}} \right)^{e_{wo}}, \qquad (6)$$

$$K_{rwg} = K_{rw}^0 \left(\frac{S_w - S_{wr}}{1 - S_{wr} - S_{org} - S_{orw}} \right)^{e_{wg}} \qquad (7)$$

Capillary effects are not important for the flow of water. The exponents, e_{wo} and e_{wg} can be made functions of density such that as miscibility is reached, S_{org} tends to decrease and the relative permeabilities of water with respect to oil and gas approach each other.

Three-Phase Relative permeability: Gas. Gas is considered to be the most non-wetting phase with respect to oil and water. So K_{rg} is assumed to be a function of gas saturation only as given by Eq. 1. This implies that the isoperms will be horizontal, straight lines (if gas hysteresis is neglected) on a ternary diagram. Typical sketches of the gas isoperms are shown in Fig. 1.

Three-Phase Relative Permeability: Water. Water is considered to be non-wetting with respect to oil but wetting to gas. Water saturation both increases and decreases with respect to gas saturation during WAG floods. Because water is wetting with respect to gas, water will have little hysteresis. Water relative permeability, K_{rw} is assumed to be an arithmetic interpolation between K_{rwg} and K_{rwo} following Baker (1988) and Blunt (2000):

$$K_{rw} = \frac{S_o K_{rwo}(S_w) + S_g K_{rwg}(S_w)}{S_o + S_g}. \qquad (8)$$

This simple saturation-weighted approximation captures the basic features of water relative permeability in mixed-wet reservoirs. If either oil or gas saturation is zero, the three-phase water relative permeability equals two-phase relative permeability. Moreover, as the miscibility limit is reached, the resulting water permeability is a function of water saturation alone. Some typical isoperms are shown in Fig. 2.

Three-Phase Relative Permeability: Oil. Oil is wetting with respect to gas and water except in the microporosity. At low oil saturations and sufficiently high water saturations, oil relative permeability depends only on the oil saturation because oil is the most wetting fluid. Howover, at low water saturations, water is present in the microporosity and competes with oil for the smaller-sized pores. Thus the oil relative permeability depends on the total liquid saturation in the limit of low water and high oil saturations. For purposes of simplicity, the oil permeability is approximated as,

$$K_{ro} = Min\ (K_{row}(S_O),\ K_{rog}(S_O+S_W)). \qquad (9)$$

The first term is lower than the second term in the right hand side of Eq. 9 in most of our simulations. Typical sketches of oil relative permeability are shown in Fig. 3.

Four-Phase Relative Permeability. In this work, the gas phase (phase 3) and the second liquid phase (phase 4) are treated as one combined pseudo-phase (g). The properties of the combined pseudo-phase is calculated and then divided between phases 3 and 4 based on their saturations as follows:

$$S_g = S_3 + S_4 \qquad (10)$$

$$g = (\rho_3 * S_3 + \rho_4 * S_4)/S_g \qquad (11)$$

$$K_{r3} = K_{rg}\ (S_g) * S_3\ /\ (S_3 + S_4) \qquad (12)$$

$$K_{r4} = K_{rg}(S_g) * S_4\ /(S_3 + S_4) \qquad (13)$$

In Guler *et al.* (2001) model, a similar approach was applied; however, the second liquid was combined with oil. That approach would decrease the importance of the nonlinearity in relative permeability because many cells contained water, oil and second liquid in our case studies. The new relative permeability model was incorporated into simulator UTCOMP.

Outline of Case Studies. Table 1 shows compositions for Schrader live oil, PBG, and NGL. Guler *et al.* (2001) provide the fluid characterization for compositional simulation. The C7+ composition was modeled by five pseudocomponents. UTCOMP (Chang et al., 1990) was used to simulate the slim tube experiments; conditions are listed in Table 2. Simulations were run using different relative permeability models and their effects on the results were analyzed. Compositional simulations were carried out for field WAG injections in a quarter 5-spot with the best solvent found from slim tube simulations. Table 3 lists the field conditions. We have doing literature search on horizontal wells. We are also designing a laboratory-scale quarter 5-spot model. Experiments will be conducted next year to evaluate the numerical models.

Results and Discussion

Relative Permeability Formulation Effect. Oil recoveries for 100% CO2 and 85% CO2-15% NGL from the Guler *et al.* (2001) model is compared with their counterparts from the new model in Fig. 8, which indicates that the new model is more conservative than the Guler *et al.* (2001) model in the prediction of oil recoveries. Table 4 shows the parameters in the relative permeability models. Fig. 5 shows that the values of oil relative permeabilities from the new model are lower than their counterparts from the Guler *et al.* model because the new model represents a more oil-wet rock. The difference in oil recovery is higher for 100% CO2 injection because it is more immiscible than the other injectant.

WAG. 1D simulations of solvent flooding suggest that two mixtures (85% CO2-15% NGL and 60% PBG-40% NGL) reach miscibility with Schrader viscous oil in situ. WAG simulations were conducted with the mixture of 85% CO2-15% NGL as the solvent. Simulations were run for both lab and field cases.

Laboratory cases. Laboratory experiments are usually carried out before the field tests for reducing risk. We have simulated a few laboratory-scale, 1D WAG displacements which can be the basis for future experiments. The WAG ratio was set to be 1. Two different slug sizes were applied: 0.1 and 0.3 PV.

Initial reservoir pressure was set at 1300 psi. Figs. 9 and 10 show the saturation-paths at 0.60 PVI for these two cases. Although at 0.60 PVI, we have injected 0.3 PV of water and 0.3 PV of solvent for both cases, the two saturation-paths are quite different. Smaller slug size increases the water saturation higher earlier. For example, at 0.3 PVI, 0.1 PV of water was injected for 0.1 PV slug size while no water was injected if 0.3 PV slug size is used. The saturation paths developed in this study can be used as guides for future relative permeability experiments.

Field Cases. For field cases, effects of both WAG ratios and slug sizes on oil recovery were investigated. WAG was performed on a reservoir by using a 20-acre five-spot pattern. Due to symmetry, only one quarter of the pattern was studied in the simulations. A $20 \times 20 \times 1$ grid was used in the simulations. Thus, gravitational effects are totally neglected.

Homogeneous Cases. Conditions of the field WAG cases are listed in Table 3, which shows the reservoir is homogeneous with a permeability of 250 md.

First, the effect of WAG ratio was investigated. While slug size was set as a constant (0.05 PV), four WAG ratios were used: 0.5, 1, 2, and 4. The total amount of solvent injected was kept at 0.5 PV in these simulations. Water, oil, gas, and the second non-aqueous liquid saturations at 0.5 PVI for the WAG ratio of 0.5 are shown in Fig. 11, which indicates the gas phase exists only

in several grid blocks on the flanks of the displacement front, similar to what was observed from slim tube simulations. The second liquid phase is present in most of the swept grid blocks. Injection of water increases the sweep of the second phase liquid, but it still breaks though the production well fairly early. Oil saturation profile at 0.5 PVI for the WAG ratio of 4 is shown in Fig. 12. It can be compared with that of Fig. 11 (b). As WAG ratio increases, solvent breakthrough is delayed in terms of cumulative (total) injection. Oil recovery is shown in Fig. 13, which indicates that oil recovery is faster with decreased WAG ratio. More solvent is injected for a lower WAG ratio than for a higher WAG ratio at any given time because of the WAG schedule and lower resistance to flow. Miscible solvent is more effective than water in recovering oil. The ultimate recovery at 0.5 PV injection of solvent is very similar. Economical analysis can be conducted to find the optimum WAG ratio.

Second, the effect of slug size on oil recovery was investigated. While WAG ratio was kept constant (0.5), slug size was varied: 0.0125 PV, 0.025 PV, 0.05 PV, and 0.1 PV. The total amount of solvent injected was kept at 0.5 PV in these simulations. The resulting oil recovery is shown in Fig. 14, which indicates that oil is recovered faster with increased slug size although the differences are not large. The increased oil recovery is due to the increase of solvent injected at a certain time as slug size increases.

Third, WAG simulations were run for two relative permeability models: the Guler *et al.* (2001) model and the new model. Oil recovery is shown in Fig. 15, which indicates that oil recovery predicted by using the new model proposed in this paper is higher than that from the Guler *et al.* model. This finding is quite the opposite of the observation from the slim tube simulations (Fig. 8). In the field simulations, injection and production pressures were kept constant. The water relative permeability is higher in the new model. That leads to a higher injectivity and thus a higher oil recovery in the new model.

Heterogeneous. By using a Dykstra-Parsons coefficient of 0.5, an average permeability of 250 md, and a dimensionless correlation length of 0.5, a heterogeneous permeability field was generated as shown in Fig. 16. Conditions other than permeabilities are the same as those used for the homogeneous cases, as shown in Table 3. Simulations for a constant slug size (0.05 PV) and varied WAG ratios (0.5, 1, 2, and 4) were run for this heterogeneous quarter five-spot. Results are shown in Fig. 17, which indicates that as WAG ratio increases, oil recovery decreases, similar to what was observed from the homogenous reservoir. Note that fluids are injected and produced faster in the heterogeneous field compared with the homogeneous field. The oil recoveries are, however, similar. The injected fluids find the higher permeability regions to move through the pattern faster than the homogeneous case.

The field simulations were run in 2D ignoring gravitational effects that are extremely important in these WAG floods. The spatial resolution is very low in the above simulations, thus leading to severe numerical dispersion. It is prohibitively time-consuming to run multi-dimensional, compositional simulations with four fluid phases on fine grids in our present simulator. We are developing our compositional streamline simulator. Waterflood and gasflood can be run in this simulator using characteristic solutions along streamlines. This scheme does not work for WAG floods. Therefore, we are developing numerical solution along the streamlines. This development will take another 3 months. We hope this simulator can turn high-resolution compositional simulation into reality.

Technology Transfer

We have submitted two papers to SPE Fall conference on the basis of this work.

Conclusions

- Effect of relative permeability, WAG ratio and slug size has been studied for quarter 5-spot WAG flood. Oil was recovered faster with increased slug size, decreased WAG ratio and the new relative formulation. Compositional streamline simulator is being developed for accurate simulation of WAG floods (Task 3).

- Effect of horizontal wells on reservoir sweep and model quarter 5-spot experimental design have been initiated (Tasks 4 and 5).

Plans for Next Reporting Period

- Streamline modeling for WAG flood (Task 3)

- Evaluate effect of complex well-architecture (Task 4)

- Design of model quarter five-spot experiments (Task 5)

References

Baker, L.E.: "Three-Phase relative Permeability Correlations," paper SPE 17369 presented at the 1988 SPE/DOE Enhanced Oil Recovery Symposium, Tulsa OK, April 17-20.

Bidinger, C. R. & Dillon, J. F., "Milne Point Shrader Bluff: Finding the Keys to Two Billion Barrels," SPE 30289, International Heavy Oil Symposium, Calgary, June 19-21, 1995.

Blunt, M.J.: "An empirical Model for Three-Phase Relative Permeability", paper SPE 67950, *SPEJ* (Dec. 2000), 435-445.

Chang, Y., Pope, G. A. and Sepehrnoori, K., "A Higher Order Finite-Difference Compositional Simulator," J. Petrol. Sc. & Eng., 5, 35-50, 1990.

Foerester, C. et al., "West Sak Field Development: Analysis of a Marginal Project," SPE 37946, *SPE Hyd. Econ. & Eva.*, Dallas, March 16-18, 1997.

Guler, B. *et al.*: "Three- and Four-Phased Flow Compositional Simulations of CO_2/NGL EOR," paper SPE 71485 presented at the 2001 SPE Annual Technical Conference and Exhibition held in New Orleans, LA, Sept. 30-Oct. 3.

Jerauld, G.R.: "General Three-Phase Relative Permeability Model for Purdhoe Bay", *SPERE* (Nov. 1997), 255-263.

Land, C.S.: "Calculation of Imbibition Relative Permeability for Two- and Three-Phase Flow from Rock Properties", *SPEJ* (June 1968) 149; *Trans.*, AIME, 243.

Table 1 - Schrader Fluid Compositions			
Component	Live Oil	PBG	NGL
CO_2	0.000436	0.12179	0
C1	0.272149	0.76587	0
C2	0.004128	0.06242	0
C3	0.010484	0.03133	0.0439
C4	0.021230	0.01108	0.4337
C5	0.020020	0.00329	0.2543
C6	0.022566	0.00422	0.1198
C7-9	0.098746	0	0.1483
C10-13	0.100533	0	0
C14-19	0.145138	0	0
C20-35	0.164159	0	0
C36P	0.140411	0	0

Table 2 - Conditions for the Slim Tube Experiments[2]		
Parameters	Value	Unit
P_i	1300	psi
T	82	^{o}F
K	5000	md
ϕ	0.352	unitless
D	0.252	in
L	40	ft

Table 3 - Conditions for the Field WAG Cases		
Parameter	Value	Unit
$X_{1/4}$	466.6905	ft
$Y_{1/4}$	466.6905	ft
Z	1	ft
S_{wi}	0.4	unitless
K_x	250	md
K_y	250	md
K_z	250	md
$\underline{T}$	86	^{o}F
P_i	1750	psi
ϕ	0.352	unitless
P_{inj}	1800	psi
P_{pro}	900	psi

Table 4 - Dimensionless Parameters Used to Compare the Guler *et al*. and New Models	
S_{org}, S_{orw}	0.2
S_{wr}	0.25
S_{gr}	0.05
K_{ro}^{0}	0.71
K_{rw}^{0}	0.21
K_{rg}^{0}	1
C_{ow}, C_{og}	2.5
e_{wo}, e_{wg}	1.5
C_{g1}	2.5
C_{g2}	0
b	0
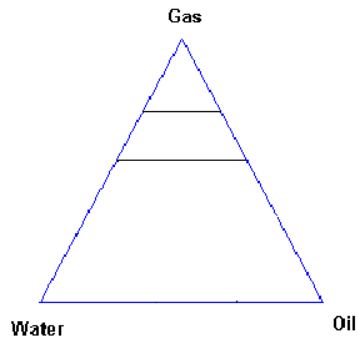
Fig. 1 - Isoperm sketches of gas relative permeability in a three-phase system.
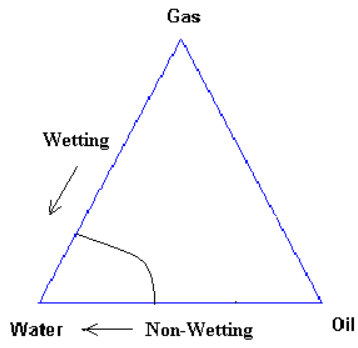
Fig. 2 - Isoperm sketches of water relative permeability in a three-phase system.
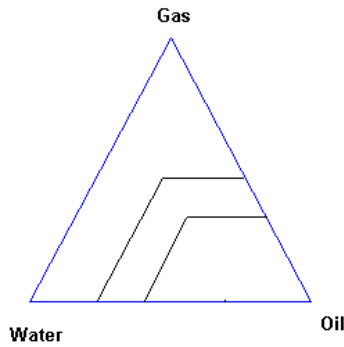
Fig. 3 - Isoperm sketches of oil relative permeability in a three-phase system.
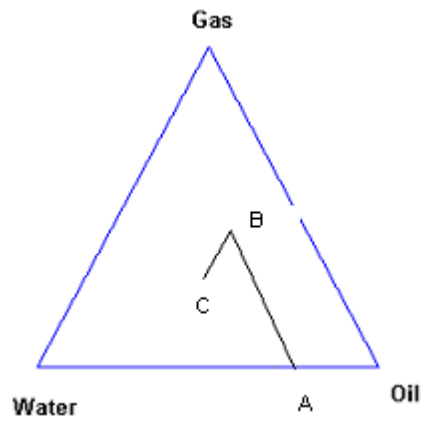
Fig. 4 - Saturation path in a three-phase system.
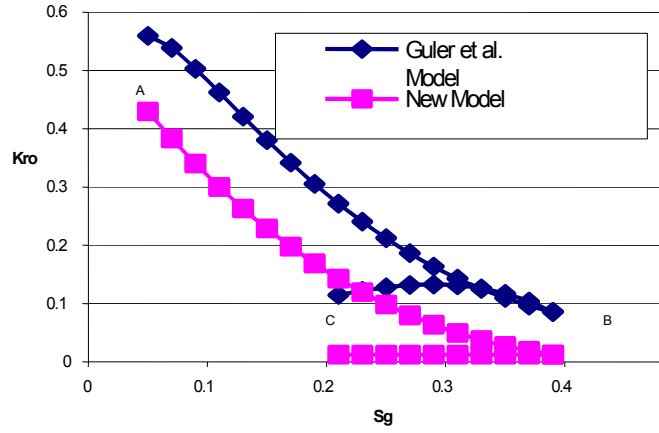
Fig. 5 - Comparision of oil relative permeabilitity from the Guler *et al.* and new relative permeability models.

Fig. 6 - Comparision of water relative permeabilitity from the Guler *et al.* and new relative permeability models.

Fig. 7 - Comparision of gas relative permeability from the Guler *et al.* and new relative permeability models.

22
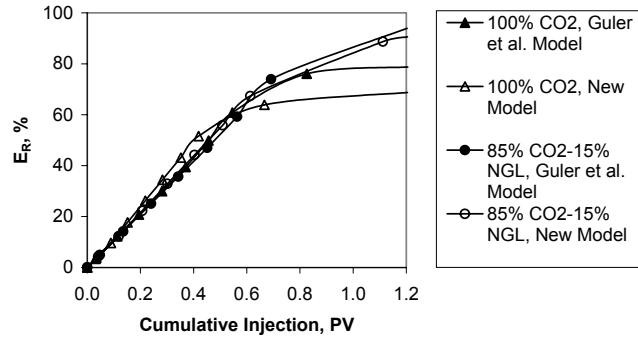
Fig. 8 - Oil recoveries at various times for 100% CO2 and 85% CO2 plus 15% NGL injections by using the Guler *et al.* and new relative permeability models.

Fig. 9 - Saturatrion path for 1D WAG (1:1, slug = 0.3 PV) at 0.60 PVI.
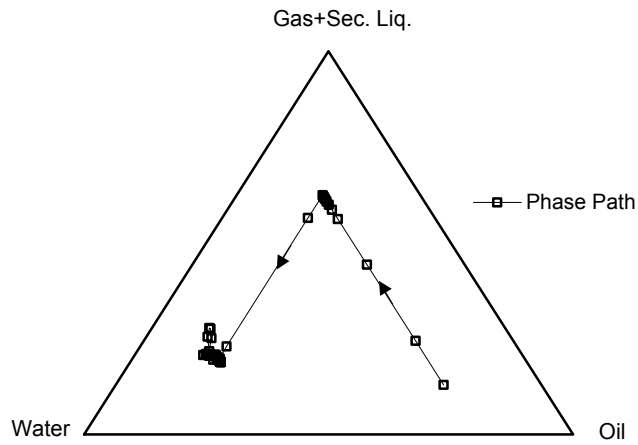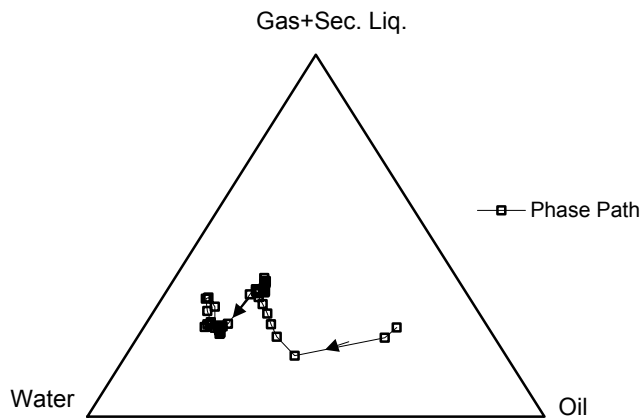
Fig. 10 - Saturation path for 1D WAG (1:1, slug = 0.1 PV) at 0.60 PVI.
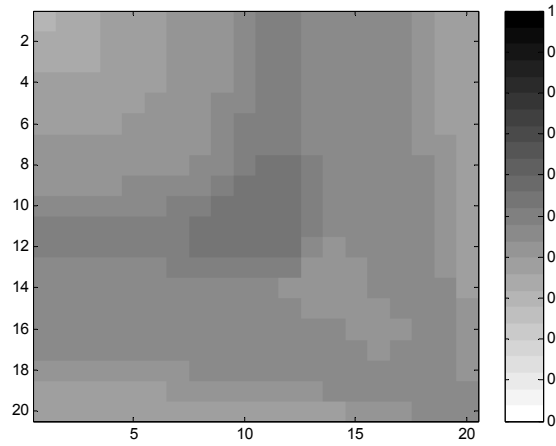
a) Water.
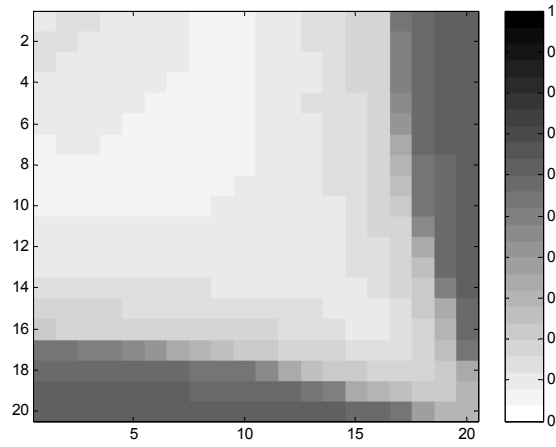
b) Oil.
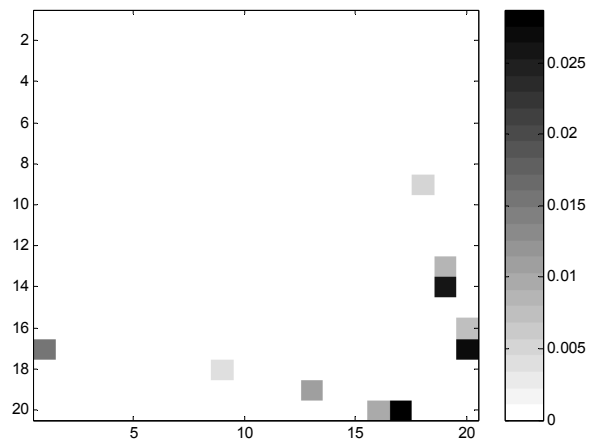
c) Gas.
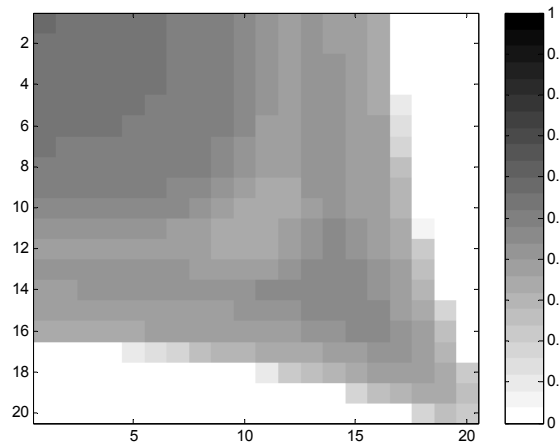
d) Second non-aqueous liquid.

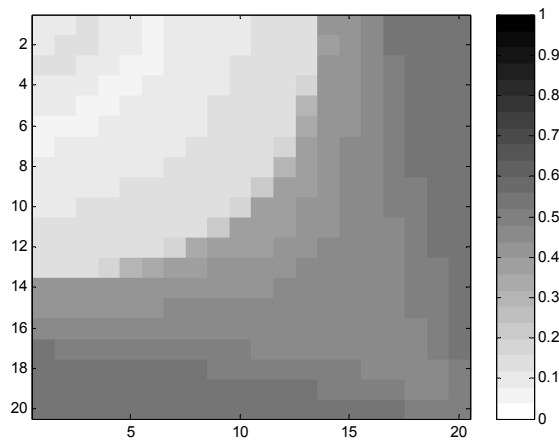Fig. 11 - Saturation profiles at 0.5 PVI for 2D homogeneous field WAG processes with a constant slug size (0.05 PV) and a WAG ratio of 0.5.

Fig. 12 - Oil saturation profiles at 0.5 PVI for 2D homogeneous field WAG processes with a constant slug size (0.05 PV) and WAG ratio = 4.
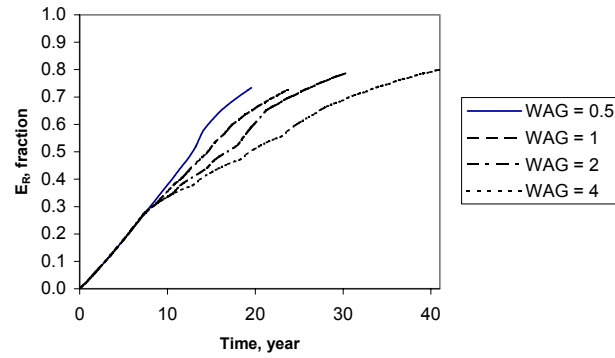
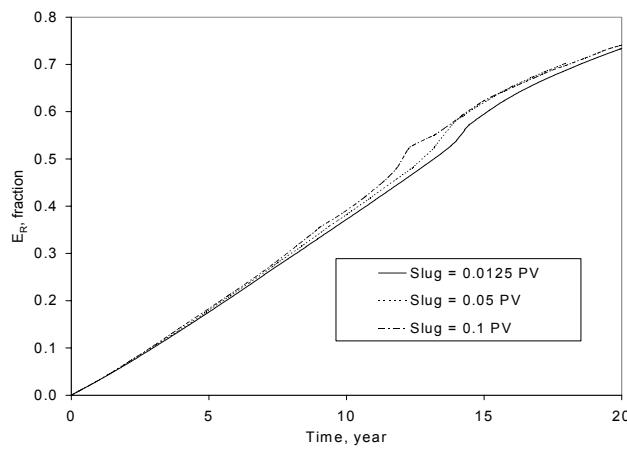Fig. 13 - Oil recoveries for 2D homogeneous field WAG processes with a constant slug size (0.05 PV) and varied WAG ratios.

Fig. 14 - Oil recoveries for 2D homogeneous field WAG processes with a constant WAG ratio (0.5) and varied slug sizes.
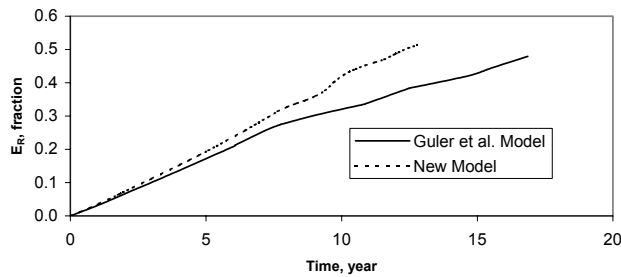

Fig. 15 - Oil recovery for WAG ratio of 2 and solvent slug size of 0.05 PV from two relative permeability models.
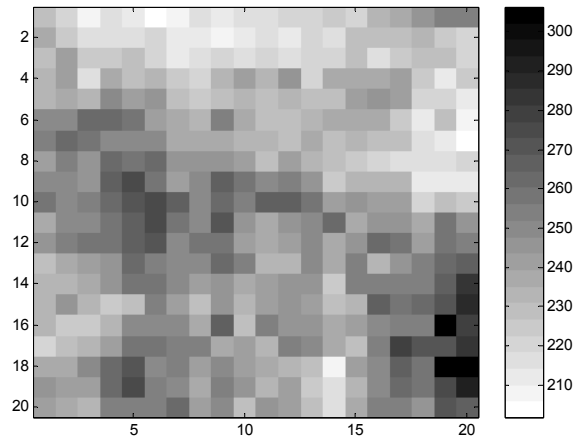
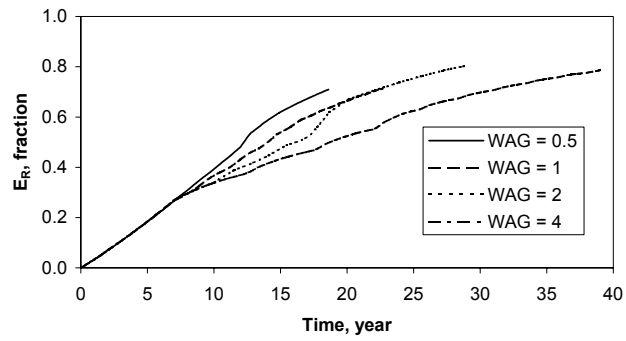Fig. 16 - Permeability distribution for a heterogeneous reservoir.

Fig. 17 - Oil recoveries for 2D heterogeneous field WAG processes with a constant slug size (0.05 PV) and varied WAG ratios.